

Incorporation of high concentrations of erbium in crystal silicon

A. Polman, J. S. Custer, E. Snoeks, and G. N. van den Hoven
FOM Institute for Atomic and Molecular Physics, Kruislaan 407, 1098 SJ Amsterdam, The Netherlands

(Received 17 August 1992; accepted for publication 30 November 1992)

High concentrations ($\approx 10^{20}/\text{cm}^3$) of Er have been incorporated in crystal Si by solid phase epitaxy of Er-implanted amorphous Si. This concentration is some 2 orders of magnitude higher than has previously been achieved. During thermal recrystallization of the amorphous layer, segregation and trapping of Er occurs at the moving crystal/amorphous interface. As long as the concentration of Er trapped in the crystal remains below a critical level, perfect epitaxial regrowth occurs. This concentration limit is temperature dependent, decreasing from $1.2 \pm 0.2 \times 10^{20}/\text{cm}^3$ at 600 °C to $6 \pm 2 \times 10^{19}/\text{cm}^3$ at 900 °C.

Silicon would be the material of choice for optoelectronic technology if efficient light emission could be achieved. Unfortunately, because of its indirect band gap, Si has very inefficient band-to-band luminescence under electrical excitation. Several attempts have been made to avoid this problem, such as band-gap engineering by the addition of Ge, or the addition of isoelectronic impurities or structural defects causing radiative recombination, but so far these techniques have not proven successful. More recently, Ennen *et al.* pointed out the potential of rare-earth ions in semiconductors.^{1,2} Rare-earth ions in the correct charge state, exhibit luminescent intra- $4f$ transitions, which are shielded from the surrounding medium by filled outer electron shells. Erbium is of interest because these transitions occur near 1.5 μm , a wavelength of great importance in optical communication technology.

Erbium-doped Si will only be useful, however, if enough Er can be incorporated in crystal Si (*c*-Si) and made optically active. Ion implantation followed by thermal annealing is the usual method to introduce Er into Si.¹⁻⁸ While low concentrations of Er ($< 1 \times 10^{18}$ Er/cm³) can be implanted and activated in single-crystal Si, high-dose implants lead to one of two problems. First, above a critical Er dose ($2 \times 10^{13}/\text{cm}^2$ at 500 keV), while still below the amorphization limit, high-temperature annealing leads to extended defect formation.⁶ Although this was suggested to be caused by the solubility limit of Er in Si, the observed defect structures are very similar to preamorphization damage (dislocations formed by agglomeration of displacement damage) which should also occur in this dose range.⁹ Second, above the amorphization limit, attempting to epitaxially recrystallize the Er doped amorphous Si with high-temperature (> 750 °C) anneals generally results in poor crystal quality.⁴⁻⁶

In this letter we demonstrate how to incorporate up to 10^{20} Er/cm³ in high-quality *c*-Si, more than 2 orders of magnitude more Er than has been previously achieved. Erbium is implanted to form a fully amorphized silicon (*a*-Si) surface layer. During recrystallization of the *a*-Si by thermal solid phase epitaxy (SPE), segregation and trapping of Er occurs at the moving *c*-Si/*a*-Si interface. Only within certain concentration and temperature windows are high concentrations of Er trapped in high quality single-crystal Si.

Erbium was incorporated in *a*-Si by either implanting

Er directly into *c*-Si ($4 \times 10^{14}/\text{cm}^2$ and $9 \times 10^{14}/\text{cm}^2$ 250 keV Er) or into *a*-Si previously made by Si implantation ($3 \times 10^{15}/\text{cm}^2$ 350 keV Si followed by 1.3, 2.4, or $5.4 \times 10^{15}/\text{cm}^2$ 250 keV Er). All implants were performed with the samples heat sunk to a copper block cooled by liquid nitrogen. The amorphous layer thicknesses and Er concentration profiles were measured with Rutherford backscattering spectrometry (RBS) using 2 MeV He. The backscattering angle was 100°, giving a depth resolution of 10 nm for a surface barrier detector cooled to 0 °C (16 keV resolution). The low-dose Er implants generated amorphous layers 140–160 nm thick, while the Si preamorphized layers were 500 nm thick. The as-implanted Er profiles were approximately Gaussian and peaked at a depth of 70 nm with a FWHM of 60 nm. Thermal anneals were done in a rapid thermal annealer (RTA) under flowing argon. The indicated anneal times are those after the actual anneal temperature was reached; the heat-up time was 5 s in each case.

Figure 1 shows RBS/channeling spectra for the 9×10^{14} Er/cm² sample both as-implanted and after annealing for either 15 min at 600 °C or 15 s at 900 °C. The high-yield Si region for the as-implanted sample shows the 160 nm thick *a*-Si surface layer. After annealing at 600 °C, the *a*-Si layer has epitaxially recrystallized, leaving a thin disordered layer (~ 10 nm) at the surface. The channeling minimum yield in the recrystallized layer is $\chi_{\text{min}} < 5\%$, indicating good crystal quality. The Er has been redistributed, with 65% of the Er remaining trapped in *c*-Si and the remainder in the surface disordered layer. The Er profiles are identical under both channeling and random conditions, so the Er is not on substitutional lattice sites. During 900 °C annealing, the initial regrowth is epitaxial, but 60 nm from the surface the quality of the regrown crystal deteriorates rapidly. In the epitaxial region (deeper than 60 nm), Er is trapped at concentrations similar to those for the 600 °C anneal. Once damaged crystal growth begins, Er starts being trapped at higher concentrations. The sample is recrystallized to the surface as evidenced by both the redistribution of some Er to the surface and the moderate channeling in the Si signal.

Figure 2 shows TEM micrographs confirming the RBS/channeling data of Fig. 1. Figure 2(a) shows the sample regrown at 600 °C, with an additional 15 s, 1000 °C anneal to optically activate the Er. There are no observable

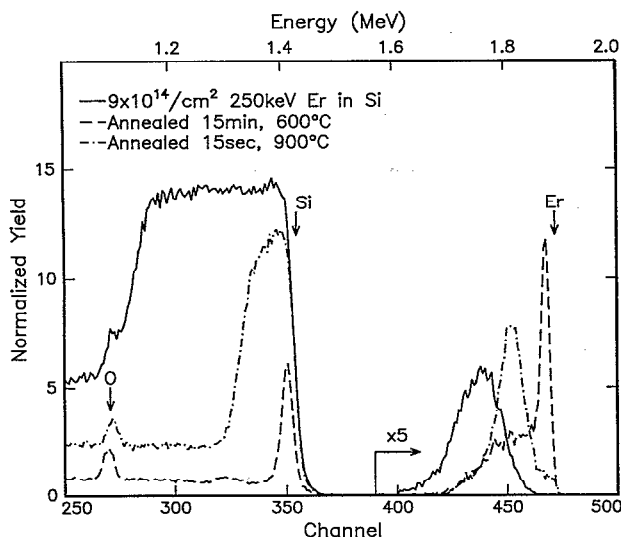


FIG. 1. RBS channeling spectra for $9 \times 10^{14}/\text{cm}^2$ 250 keV Er implanted samples as-implanted (solid line), after a 15 min 600°C anneal (dashed line), and after a 15 s 900°C anneal (dot-dashed line). The surface channels for Er, Si, and O are indicated.

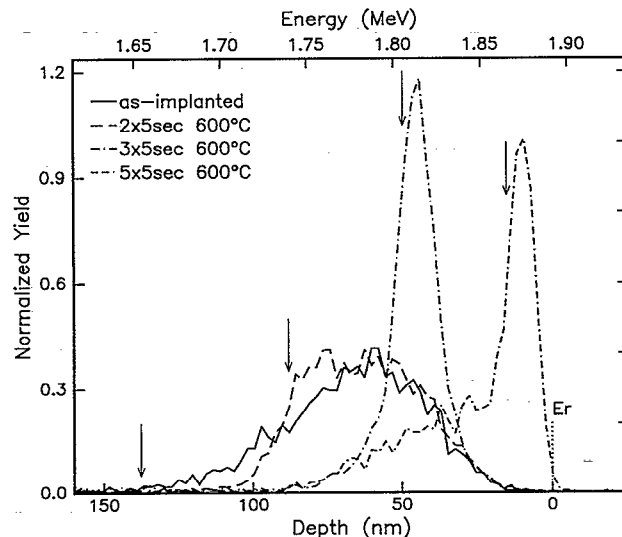


FIG. 3. RBS spectra of the 9×10^{14} Er/ cm^2 sample as-implanted, and after 2, 3, or 5 s RTA anneals of 5 s each at 600°C . The arrows indicate the position of the *c*-Si/*a*-Si interface as determined from the Si portion of each spectrum.

defects in the recrystallized layer, except within the 10 nm surface disordered layer. High resolution lattice images (not shown) show no evidence of precipitates or second-phase inclusions. Figure 2(b) shows that the top 60 nm of the 900°C annealed sample is heavily twinned *c*-Si, which causes the high yield in the RBS channeling spectrum.

The redistribution of Er during SPE is a result of segregation and trapping at the *c*-Si/*a*-Si interface. Figure 3 shows the Er portion of RBS spectra of the 4×10^{14} Er/ cm^2 sample epitaxially regrown at 600°C for different numbers of RTA anneals of 5 s each. With increasing number of anneal steps, the *c*-Si/*a*-Si interface sweeps through the as-implanted Er profile, accumulating Er in a segregation spike at the moving interface. The width of this peak is detector resolution limited, so the concentration of Er at the interface cannot be directly determined. As the Er accumulates in the spike, the amount trapped in the crystal

also increases. Once the *c*-Si/*a*-Si interface nears the surface, the amount of Er in the segregation spike decreases because there is no more Er ahead of the interface to be segregated.

The width of the segregation spike can be estimated from classical segregation theory as the ratio of the impurity diffusivity (D) ahead of the interface and the interface velocity (v). From the Si parts of the channeling spectra in Fig. 3, we obtain $v \approx 5$ nm/s. Attempts to measure D in bulk *a*-Si place an upper limit of $D < 1 \times 10^{-17}$ cm^2/s at 600°C .¹⁰ Together these yield an estimated segregation spike width < 0.0002 nm, far less than an interplane spacing, which is completely unphysical. However, the diffusivity of Er may be enhanced near the *c*-Si/*a*-Si interface, which has been previously suggested to occur for Sb and Ga.¹¹ In any case, this estimate indicates that all the segregated Er is confined at or very near the *c*-Si/*a*-Si interface, leading to Er concentrations at the interface of 10 at. % or more. Such a metal-rich environment could indeed locally increase the Er diffusivity.

The recrystallization process is sensitive not only to the anneal temperature (Fig. 1), but also to the amount of Er. Figure 4 presents RBS/channeling spectra for each Er dose after annealing for 15 min at 600°C . The Si portion [Fig. 4(a)] shows that the two lowest fluence Er samples exhibit good epitaxy with $\chi_{\text{min}} < 5\%$. The higher concentration samples all initially regrow epitaxially, but for each sample epitaxy is disrupted at a certain depth (indicated by arrows). The higher the Er dose, the sooner epitaxial growth is disrupted. Figure 4(b) shows the Er parts of the RBS spectra plotted on the same depth scale as for the Si parts. The two low-fluence samples have Er profiles as shown in Fig. 1, with Er trapped in high-quality crystal and a narrow Er peak at the surface. The high-dose samples all show rapid increases in Er concentration once epitaxy is disrupted. Comparison of the Er concentrations for each sam-

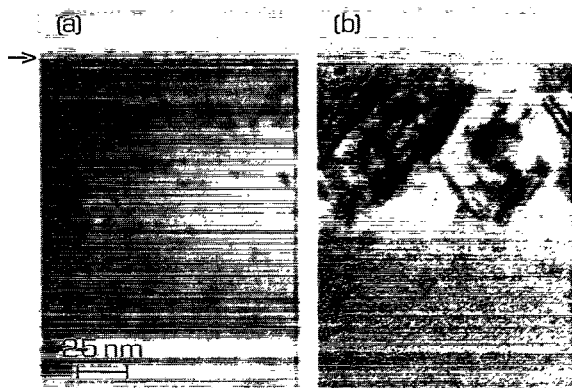


FIG. 2. TEM micrographs of $9 \times 10^{14}/\text{cm}^2$ 250 keV Er implanted samples after (a) a 15 min 600°C regrowth anneal followed by a 15 s 1000°C anneal for optical activation, and (b) after a single-step 15 s 900°C anneal. The surface is indicated by an arrow.

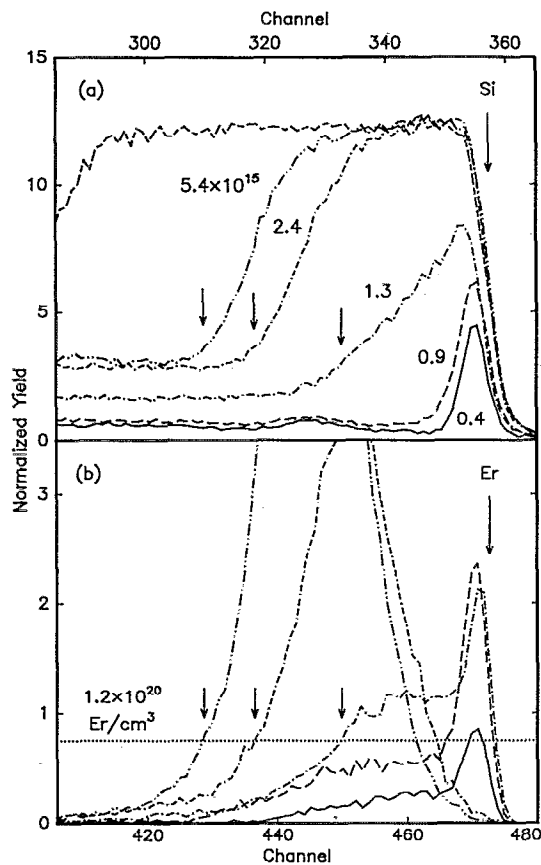


FIG. 4. The Si (a) and Er(b) portions of RBS spectra after 15 min, 600 °C anneals of samples implanted with $0.4, 0.9, 1.3, 2.4,$ and $5.4 \times 10^{15}/\text{cm}^2$ 250 keV Er. The channel scales are plotted such that Si and Er have the same relative depth scale. The dotted line in (b) indicates the critical Er concentration where epitaxy is disrupted.

ple at the depth where single-crystal regrowth is interrupted (indicated by arrows) demonstrates that epitaxy is disrupted once a fixed Er concentration in the crystal, $1.2 \pm 0.2 \times 10^{20}/\text{cm}^3$, is reached. Similar analysis of regrowth at 900 °C yields a lower trapped Er concentration limit of only $6 \pm 2 \times 10^{19}/\text{cm}^3$, with only the lowest fluence Er sample regrowing completely.

The behavior of Er during SPE is reminiscent of that of several other impurities. The (unexpected) segregation of a slow-diffusing element is similar to the case of In.¹² However, at high enough In concentrations, an amorphous to polycrystal transformation occurs that apparently is liquid mediated.¹³ This is unlikely for a high-melting temperature element such as Er. Instead, high enough Er concentrations at the *c*-Si/*a*-Si interface result in twin formation, similar to what is observed during SPE of Au doped *a*-Si.¹⁴ However, unlike Er, no measureable amount of Au is trapped in the crystal before twin formation.

We have demonstrated here that the segregation and trapping behavior of Er during SPE is sensitive to the regrowth temperature and the Er concentration. This explains why earlier attempts to use SPE to incorporate high concentrations of Er in defect-free crystal have failed,³⁻⁶ generally because too high a temperature was used during recrystallization in an attempt to optically activate the Er

in the same anneal step. Although we observe some photoluminescence in samples regrown at 600 °C, the intensity can be increased greatly by high-temperature, post-regrowth RTA anneals, with the best results obtained after a 15 s, 1000 °C anneal.¹⁰ These samples have sharply peaked photoluminescence spectra, measured at 77 K, centered around $1.55 \mu\text{m}$, similar to previous experiments.^{2,3,8} The crystal quality of these samples remains good, as demonstrated by the TEM micrograph in Fig. 2.

In conclusion, we have incorporated up to $10^{20} \text{Er}/\text{cm}^3$ in high-quality *c*-Si, some 2 orders of magnitude more than has been previously achieved. This was done using solid phase epitaxial regrowth of Er-doped amorphous Si at 600 °C, which is accompanied by segregation and trapping of Er at the moving *c*-Si/*a*-Si interface. High initial concentrations of Er eventually disrupt epitaxy. Higher temperature anneals (900 °C) exhibit breakdown in the epitaxy at even lower initial concentrations. If all of the Er incorporated in the *c*-Si could be optically activated, the fabrication of Si-based optical devices such as light emitting diodes and optical amplifiers would be feasible.

We would like to thank H. Zandbergen and F. D. Tichelaar (Delft University of Technology) for assistance with high-resolution TEM. This work is part of the research program of FOM and was made possible by financial support from NWO, STW, and IOP Electro-Optics.

- ¹ H. Ennen, J. Schneider, G. Pomrenke, and A. Axmann, *Appl. Phys. Lett.* **43**, 943 (1983).
- ² H. Ennen, G. Pomrenke, A. Axmann, K. Eisele, W. Haydl, and J. Schneider, *Appl. Phys. Lett.* **46**, 381 (1985).
- ³ D. Moutonnet, H. L'Haridon, P. N. Favennec, M. Salvi, M. Gauneau, F. Arnaud D'Avitaya, and J. Chroboczek, *Mater. Sci. Eng. B* **4**, 75 (1989).
- ⁴ Y. S. Tang and Z. Jingping, *J. Cryst. Growth* **102**, 681 (1990).
- ⁵ W. P. Gillin, Z. Jingping, and B. J. Sealy, *Solid State Commun.* **77**, 907 (1991).
- ⁶ D. J. Eaglesham, J. Michel, E. A. Fitzgerald, D. C. Jacobson, J. M. Poate, J. L. Benton, A. Polman, Y.-H. Xie, and L. C. Kimerling, *Appl. Phys. Lett.* **58**, 2797 (1991).
- ⁷ J. L. Benton, J. Michel, L. C. Kimerling, D. C. Jacobson, Y.-H. Xie, D. J. Eaglesham, E. A. Fitzgerald, and J. M. Poate, *J. Appl. Phys.* **70**, 2667 (1991).
- ⁸ J. Michel, J. L. Benton, R. F. Ferrante, D. C. Jacobson, D. J. Eaglesham, E. A. Fitzgerald, Y.-H. Xie, J. M. Poate, and L. C. Kimerling, *J. Appl. Phys.* **70**, 2672 (1991).
- ⁹ R. J. Schreutelkamp, J. S. Custer, J. R. Liefting, W. X. Lu, and F. W. Saris, *Mater. Sci. Rep.* **6**, 275 (1991).
- ¹⁰ A. Polman, J. S. Custer, E. Snoeks, and G. N. van den Hoven (unpublished).
- ¹¹ W. F. J. Slijkerman, J. M. Gay, P. M. Zagwijn, J. F. van der Veen, J. E. Macdonald, A. A. Williams, D. J. Gravesteijn, and G. F. A. van de Walle, *J. Appl. Phys.* **68**, 5105 (1990); P. M. Zagwijn, Y. N. Erokhin, W. F. J. Slijkerman, J. F. van der Veen, G. F. A. van de Walle, D. J. Gravesteijn, and A. A. van Gorkum, *Appl. Phys. Lett.* **59**, 1461 (1991).
- ¹² J. S. Williams and R. G. Elliman, *Nucl. Instrum. Methods* **182/183**, 389 (1981).
- ¹³ E. Nygren, A. P. Pogany, K. T. Short, J. S. Williams, R. G. Elliman, and J. M. Poate, *Appl. Phys. Lett.* **52**, 439 (1988).
- ¹⁴ D. C. Jacobson, J. M. Poate, and G. L. Olson, *Appl. Phys. Lett.* **40**, 118 (1986).